Geophysical Journal International

Geophys. J. Int. (2012) **191,** 1129–1134 doi: 10.1111/j.1365-246X.2012.05703.x

An enigma in estimates of the Earth's dynamic ellipticity

E. Morrow,[1] J. X. Mitrovica,[1] A. M. Forte,[2] P. Glišović[2] and P. Huybers[1]

[1] *Department of Earth and Planetary Sciences, Harvard University,* 20 *Oxford Street, Cambridge, MA* 02138*, USA. E-mail: emorrow@fas.harvard.edu*
[2] *GEOTOP, Université du Québec à Montréal, CP* 8888 *Succursale Centre-Ville, Montréal, QC H3C 3P8, Canada*

Accepted 2012 September 28. Received 2012 August 7; in original form 2012 January 18

SUMMARY

The precession and obliquity frequencies of the Earth's rotational motion are functions of the dynamic ellipticity of the Earth's gravitational figure, and this connection has provided a novel bridge between studies of palaeoclimate and geodynamics. In particular, analyses of tuned climate proxy records have yielded bounds on the mean relative perturbation in dynamic ellipticity over both the last 3 Myr and 25 Myr that are less than ∼3 per cent of the non-hydrostatic component of the ellipticity. We demonstrate that this apparent consistency actually defines an important geophysical enigma. Over the last 3 Myr, changes in the Earth's figure are likely dominated by ice age forcings—in this case, a small perturbation to dynamic ellipticity implies significant isostatic compensation of the ice-ocean surface mass loads and, hence, a relatively low mantle viscosity. In contrast, over the last 25 Myr, changes in the Earth's long-wavelength gravitational form are likely dominated by mantle convective flow, and in this case, the small perturbation to dynamic ellipticity implies sluggish convection and a relatively high mantle viscosity. There are at least four possible routes to resolving this enigma: The viscosity in the Earth's mantle is transient (i.e. dependent on the timescale of the applied forcing), tidal dissipation changed in a manner between the last 3 Myr and 25 Myr that was sufficient to resolve the issue, the observationally inferred bounds are unrealistically restrictive, or earth models exist in which the ice age and convection effects approximately cancel leading to no net perturbation. In this paper, we compute a suite of numerical predictions of ice age and convection-induced perturbations to the dynamic ellipticity to illustrate the enigma described above.

Key words: Gravity anomalies and Earth structure; Earth rotation variations; Rheology: mantle.

1 INTRODUCTION

Analysis of deep-sea sedimentary cores has revealed Milankovitch band variations in a diverse suite of climate proxy records, including, for example, depth-series of elemental and isotopic ratios, organic material and magnetic susceptibility (e.g. Pälike & Shackleton 2000; Lourens *et al.* 2001; Lisiecki & Raymo 2005). Comparison of these variations with results from many-body orbital integrations (e.g. Laskar *et al.* 1993) allows these depth-series to be converted to time-series through a process termed astronomical calibration—or tuning—which has been applied to major portions of the Cenozoic timescale (Shackleton *et al.* 1990; Hilgen *et al.* 1995; Shackleton *et al.* 1999). The accuracy of the tuning procedure is a function of several factors, notably the existence of well-dated tie points within the cores, such as magnetic reversals, and the stability of Milankovitch frequencies within the precession and obliquity bands. In particular, these frequencies are functions of the dynamic ellipticity of the Earth, and there has been growing appreciation that geophysical processes, such as glacial isostatic adjustment (GIA) associated with the last ice age (Laskar *et al.* 1993; Mitrovica *et al.* 1994, 1997; Mitrovica & Forte 1995; Jiang & Peltier 1996) and thermal convection within the Earth's mantle (Forte & Mitrovica 1997) will drive non-negligible perturbations in this ellipticity. Moreover, with an eye to the geophysical implications, several studies have used palaeoclimate records obtained from marine sediment cores to place bounds on the variation of the dynamic ellipticity across timescales extending over the past 3 Myr (Lourens *et al.* 2001) and 25 Myr (Pälike & Shackleton 2000).

The dynamic ellipticity (H), or precession constant, of the Earth is defined as:

$$H = \frac{C - \frac{1}{2}(A + B)}{C}, \tag{1}$$

where C is the polar moment of inertia and A and B are principal equatorial moments of inertia. One can show that the relative perturbation in H may be written as (Laskar *et al.* 1993; Mitrovica *et al.*

1994):

$$\frac{\delta H}{H} = \frac{3}{2H}\frac{\delta C}{C}. \quad (2)$$

A related, and perhaps more physical measure of the oblateness of the planet is the flattening, f. The flattening is defined as the difference between the equatorial and polar radii of the Earth's geoid at spherical harmonic degree and order (2,0), and it is related to the perturbation in the dynamic ellipticity by:

$$f = \frac{3CH}{2M_e a}\frac{\delta H}{H} \sim 1.06 \times 10^4 \frac{\delta H}{H}, \quad (3)$$

where M_e and a are the mass and radius of the Earth, respectively, and f is in metres.

The Earth's dynamic ellipticity is dominated by the hydrostatic form, which denotes the equilibrium, fluid response of the planet to its present rotation rate. The residual, non-hydrostatic form of the Earth is characterized by an excess ellipticity of $\delta H/H = 0.011$ or, alternatively, an excess flattening of $f = 113$ m (Chambat *et al.* 2010). The excess flattening is widely thought to be driven by mantle convective flow, and specifically the distortion of the Earth's form associated with two massive plumes rising from the core–mantle boundary below Africa and the southeast Pacific (e.g. Lithgow-Bertelloni & Silver 1998) and the ring of subduction encircling the Pacific Ocean. In the following, we will denote the observationally inferred and predicted perturbations from these present-day values by $\Delta H/H$ and Δf. Furthermore, the mean value of these perturbations over a time window of 3 Myr and 25 Myr will be denoted by $\langle\rangle_{3\mathrm{Ma}}$ and $\langle\rangle_{25\mathrm{Ma}}$, respectively.

Bounds on $\langle \Delta H/H \rangle$ and $\langle \Delta f \rangle$ obtained by Lourens *et al.* (2001) and Pälike & Shackleton (2000) from the analysis of sedimentary cores are shown in Fig. 1. Lourens *et al.* (2001) measured the depth variation of a titanium–aluminum ratio within a core drilled in the eastern Mediterranean (ODP Site 967) dated to span 2.44–2.90 Ma. They compared this depth series to orbital (many-body) solutions generated for a suite of integrations in which the tidal dissipation and dynamic ellipticity were varied from their present-day values. They concluded that $0.0003 > \langle \Delta H/H \rangle_{3\mathrm{Ma}} > -0.0003$ or, equivalently, that $3.2\,\mathrm{m} > \langle \Delta f \rangle_{3\mathrm{Ma}} > -3.2\,\mathrm{m}$ (Fig. 1A). Pälike & Shackleton (2000) bounded the tidal dissipation and dynamic ellipticity over the past 25 Myr by fitting the amplitude modulation of a magnetic susceptibility record from the Ceara Rise (ODP Leg 154) interfered with a reference orbital signal to a semi-analytical approximation to the orbital solution. They concluded that $0.0004 > \langle \Delta H/H \rangle_{25\mathrm{Ma}} > -0.0001$ or, equivalently, that $4.2\,\mathrm{m} > \langle \Delta f \rangle_{25\mathrm{Ma}} > -1.1\,\mathrm{m}$ (Fig. 1B).

The apparent consistency between these bounds on the Earth's dynamic ellipticity may be misleading. The two analyses cover different timescales and, more importantly, the dominant geophysical processes that drive changes in the Earth's figure over each of these timescales may be distinct. Over the last 2–3 Myr, perturbations in the Earth's dynamic ellipticity are thought to be largely driven by GIA; that is, mass redistribution associated with the Plio-Pleistocene ice age. In this case, the bound on $\langle \Delta H/H \rangle$ obtained by Lourens *et al.* (2001) implies that the ice-age surface mass loading remained largely isostatically compensated across the glacial period and this, in turn, implies a relatively low deep mantle viscosity. In contrast, the advection of density heterogeneities and boundary deformation associated with thermal convection in the Earth's mantle are thought to dominate changes in the Earth's ellipticity over the longer, 25 Myr, timescale. In this case, the bound on $\langle \Delta H/H \rangle$ derived by Pälike & Shackleton (2000) implies sluggish mantle flow and, hence, a high deep mantle viscosity. Thus, the consistency in the bounds on $\langle \Delta H/H \rangle$ over the last 3 Myr and 25 Myr defines a potentially important enigma in our present understanding of the global scale dynamic evolution of the Earth during the Late Cenozoic.

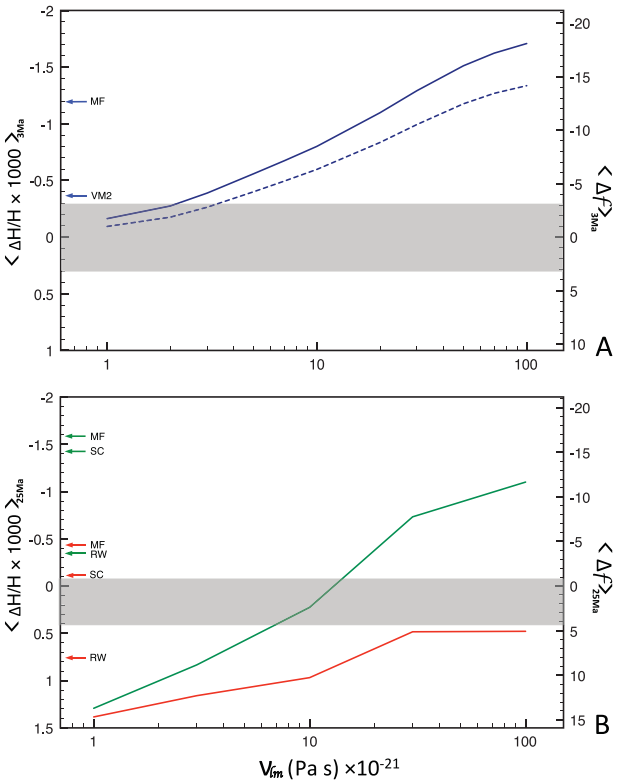

Figure 1. (A) Observationally inferred and predicted perturbations in the dynamic ellipticity over the last 3 Myr. The shaded region is the bound on the mean relative perturbation in the dynamic ellipticity inferred by Lourens *et al.* (2001) from the analysis of a sedimentary core from the eastern Mediterranean dated to span 2.44–2.90 Ma. The solid blue line is a prediction of $\langle \Delta H/H \rangle_{3\mathrm{Ma}}$ due to GIA as a function of the lower-mantle viscosity of the adopted earth model using an ice volume history inferred from the oxygen isotope record of Lisiecki & Raymo (2005) (see text). The blue arrows marked MF and VM2 are GIA predictions of $\langle \Delta H/H \rangle_{3\mathrm{Ma}}$ based on the same ice history and viscosity models MF and VM2 (see Fig. 3). The dashed blue line is identical to the solid, with the exception that ice volumes are inferred from the sea level estimate of De Boer *et al.* (2010). (B) As in frame A, except for the time span of 25 Myr. The shaded region is the associated bound on $\langle \Delta H/H \rangle_{25\mathrm{Ma}}$ derived by Pälike & Shackleton (2000) from a magnetic susceptibility record from the Ceara Rise. The red line is a numerical prediction of $\langle \Delta H/H \rangle_{25\mathrm{Ma}}$ due to mantle convection. The green line is a prediction of the total $\langle \Delta H/H \rangle_{25\mathrm{Ma}}$ due to both mantle convection and GIA. The arrows MF, RW and SC are predictions of $\langle \Delta H/H \rangle_{25\mathrm{Ma}}$ computed using the viscosity models MF, RW and SC (see Fig. 3), respectively. In this case, the red and green arrows refer to predictions including mantle convection alone and mantle convection plus GIA, respectively.

2 NUMERICAL RESULTS

2.1 Defining the enigma

To begin, we outline a suite of numerical predictions of the $\Delta H/H$ over the last 3.0 Myr due to GIA. The calculations are based on the methodology outlined in Mitrovica *et al.* (1997). We adopt a spherically symmetric, self-gravitating, elastically compressible Maxwell viscoelastic earth model with the elastic and density structure

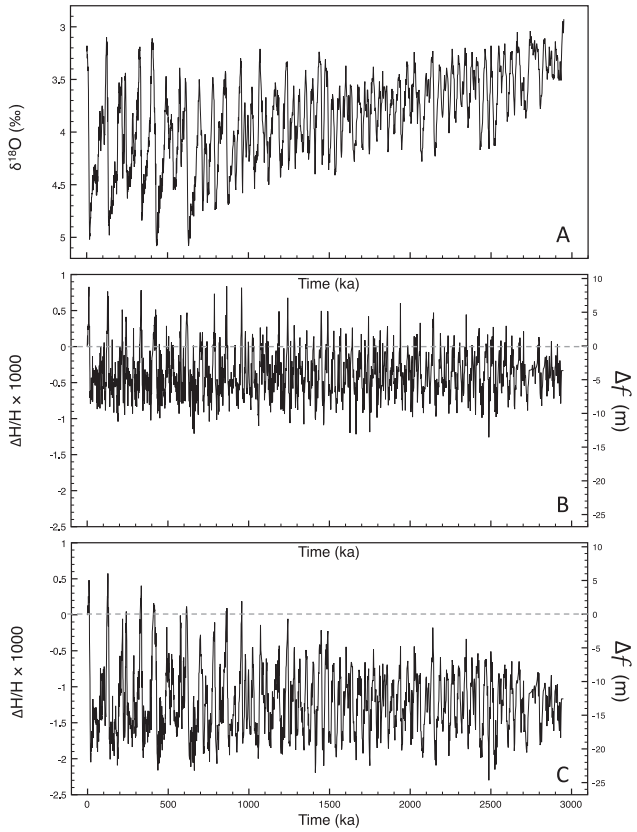

Figure 2. (A) Global stack of benthic δ^{18}O records over the last 3 Myr (Lisiecki & Raymo 2005). (B) Numerical prediction of the relative perturbation in dynamic ellipticity, $\Delta H/H$ due to GIA, based on the ice history derived from frame A (see text) and the VM2 profile of mantle viscosity (Peltier 2004). (C) As in frame B, except that the MF viscosity model is adopted (Mitrovica & Forte 2004).

prescribed from the seismic model PREM (Dziewonski & Anderson 1981). The ice model used in the calculation is constructed in a two-step procedure ultimately based on the ICE-5G model for the geometry of global ice cover during the last glacial cycle (Peltier 2004). First, we convert a global stack of oxygen isotope ratios (Lisiecki & Raymo 2005) over the past 3 Myr (Fig. 2A) into a time-series of ice volume changes relative to the present day. The scaling we adopt yields a change in ice volume from last glacial maximum (LGM) to present that matches the ICE-5G model ice history. Next, whenever the ice volume matches one of the time slices of the ICE-5G model, we adopt the ice geometry of the latter in the former. Perturbations in the dynamic ellipticity are relatively insensitive to the level of uncertainty that characterizes the mapping between oxygen isotope variations and eustatic sea level (see later). Moreover, perturbations in H reflect deformation on very long spatial scales, and therefore predictions of these perturbations are also insensitive to the detailed spatial geometry of the model ice history. In addition to the ice load, a gravitationally self-consistent ocean load is computed by solving a sea level equation that accounts for shoreline migration, changes in the extent of grounded, marine-based ice and the feedback of rotation into sea level (Kendall *et al.* 2005). One output of the sea level calculation is the time variation in the height of the geopotential that defines the sea surface; the perturbation in dynamic ellipticity is proportional to the spherical harmonic degree two zonal component of this time-series (Mitrovica *et al.* 1997).

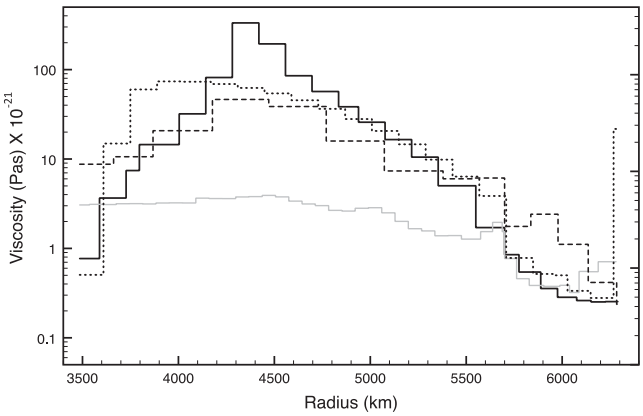

Figure 3. The four radial profiles of mantle viscosity described in the text, MF (black solid line), SC (dotted line), RW (dashed line) and VM2 (solid grey line).

Figs 2(B) and (C) show predictions of $\Delta H/H$ based on two distinct profiles of mantle viscosity, the VM2 model derived on the basis of GIA data (Peltier 2004) and model MF, which is one of a suite of models inferred from a joint inversion of GIA and mantle convection data sets (Mitrovica & Forte 2004). These models are shown in Fig. 3. Model VM2 is characterized by mean upper- and lower-mantle viscosities of $\sim 5 \times 10^{20}$ Pa s and $\sim 2 \times 10^{21}$ Pa s, respectively; analogous means for model MF are $\sim 4 \times 10^{20}$ Pa s and 2×10^{22} Pa s. The mean values of the time-series in Figs 2(B) and (C), that is, $\langle \Delta H/H \rangle_{3\mathrm{Ma}}$ are -0.37×10^{-3} ($\langle \Delta f \rangle_{3\mathrm{Ma}} = -3.9$) and -1.20×10^{-3} ($\langle \Delta f \rangle_{3\mathrm{Ma}} = -12.7$), respectively. These values are plotted as blue arrows on the left-hand side of Fig. 1(A). Both models predict perturbations in the mean dynamic ellipticity over the last 3 Myr that fall outside the range inferred by Lourens *et al.* (2001) on the basis of the core data from the eastern Mediterranean (see Fig. 1), though the misfit associated with the VM2 prediction is relatively small.

The average ice cover over the last 3 Ma is greater than in the current interglacial. Therefore, the ice age perturbation to the mean value of H over the last 3 Ma will always be negative (i.e. more mass will be concentrated at the poles during periods of glaciation than at present day), as in Figs 2(B) and (C). The magnitude of the (negative) perturbation will have a strong sensitivity to the lower-mantle viscosity (Mitrovica & Forte 1995; Mitrovica *et al.* 1997). In particular, the higher the lower-mantle viscosity, the smaller the level of isostatic compensation of the surface mass load, and the greater the ice age perturbation to the dynamic ellipticity. The mean lower-mantle viscosity in model MF is about 10 times the mean value for model VM2, and this explains the higher amplitude of the perturbation in Fig. 2(C) relative to 2(B).

The sensitivity of the GIA prediction to viscosity is systematically explored in Fig. 1(A) (solid line), where we plot values of $\langle \Delta H/H \rangle_{3\mathrm{Ma}}$ generated using a suite of earth models in which a constant lower-mantle viscosity (henceforth denoted by ν_{lm}) is varied from 10^{21} Pa s to 10^{23} Pa s. This range encompasses all geophysical estimates of ν_{lm} published in the last 40 yr. These predictions adopt a constant upper-mantle viscosity of 5×10^{20} Pa s and the ice history prescribed earlier. Over this range of lower-mantle viscosity, the mean ice age perturbation to the dynamic ellipticity increases monotonically to a value of -1.7×10^{-3} ($\langle \Delta f \rangle_{3\mathrm{Ma}} = -18.0$) as ν_{lm} is increased to 10^{23} Pa s. Most importantly, the bound on $\langle \Delta H/H \rangle_{3\mathrm{Ma}}$ inferred by Lourens *et al.* (2001) is only fit with an ice age calculation in which the lower-mantle viscosity is less than 2×10^{21} Pa s.

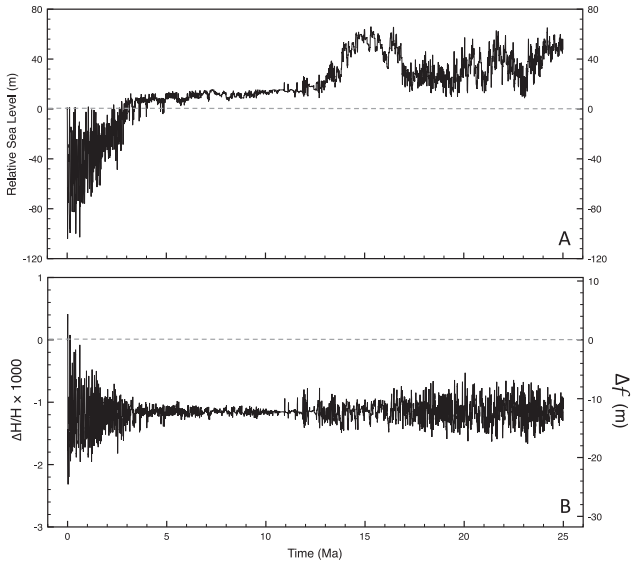

Figure 4. (A) A time-series of eustatic sea level relative to present day for the past 25 Myr compiled by De Boer *et al.* (2010). (B) Numerical prediction of the relative perturbation in dynamic ellipticity, $\Delta H/H$ due to GIA, based on the ice history derived from frame A (see text) and the MF profile of mantle viscosity (see Fig. 3)

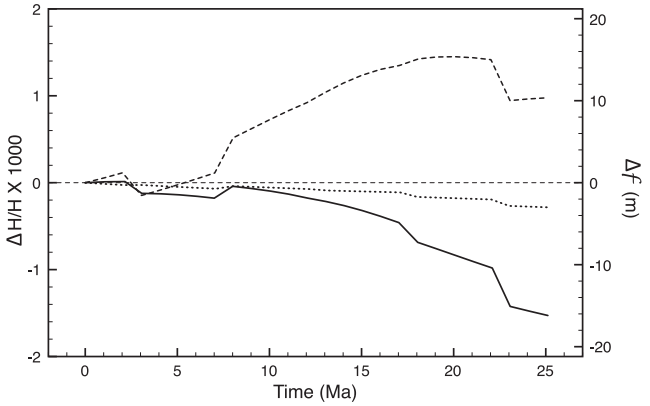

Figure 5. Numerical prediction of the relative perturbation in dynamic ellipticity, $\Delta H/H$ due to mantle convection based on the viscosity models MF (black solid line), SC (dotted line) and RW (black dashed line). Details of the calculation are described in the text.

De Boer *et al.* (2010) have inferred a time-series of eustatic sea level variations over the last 35 Myr on the basis of inverse modelling of benthic δ^{18}O records in combination with 1-D ice sheet models. We include this time-series as their results indicate that the scaling between δ^{18}O and ice volume is not constant over the past 35 Myr. The most recent 25 Myr of this time-series is shown in Fig. 4(A). The dashed line in Fig. 1(A) is analogous to the solid line with the exception that the ice history used in the prediction of $\langle \Delta H/H \rangle_{3\mathrm{Ma}}$ is constructed from the last 3 Myr of the De Boer *et al.* (2010) time-series. These results are on the order of 20 per cent smaller than those based on the ice history inferred from the time-series in Fig. 2(A). This difference is consistent with the excess ice volumes at LGM associated with these two ice histories. In particular, the ICE-5G history is characterized by a eustatic sea level change of $\sim$130 m, whereas this difference is $\sim$104 m in the time-series derived by De Boer *et al.* (2010).

Next, we turn to predictions of the perturbation in dynamic ellipticity over the last 25 Myr driven by mantle convection. These predictions adopt the tomography based flow model described in Forte *et al.* (2010) that solves the field equations valid for a compressible, Newtonian viscous fluid within a spherical shell geometry. Surface tectonic motions are coupled to the mantle flow rather than being imposed as boundary conditions (Forte 2007). The system of governing equations is backward advected 25 Myr from an initial density field derived via a joint inversion of global seismic and geodynamic data sets (Simmons *et al.* 2009). The latter includes present-day free-air gravity anomalies, surface (crust-corrected) dynamic topography, tectonic plate motions and the geodetically inferred excess ellipticity of the core–mantle boundary. The inversion is based on viscosity model MF. Fig. 5 shows time-series of $\Delta H/H$ computed using viscosity profile MF. From this time-series we obtain a mean perturbation $\langle \Delta H/H \rangle_{25\mathrm{Ma}} = -4.1 \times 10^{-4}$.

The sensitivity of the convection-induced mean perturbation, $\langle \Delta H/H \rangle_{25\mathrm{Ma}}$, to ν_{lm} is illustrated in Fig. 1(B) (red line), where, we show results for a suite of models in which ν_{lm} is varied from 10^{21} to 10^{23} Pa s. The bound derived by Pälike & Shackleton (2000) is best fit for earth models with a lower-mantle viscosity in excess of 3×10^{22} Pa s. This preference for a high-viscosity deep mantle is not surprising given that the bound on the mean perturbation in $\langle \Delta H/H \rangle_{25\mathrm{Ma}}$ or Δf derived by Pälike & Shackleton (2000) is only a few per cent of the total present-day excess ellipticity and flattening of the Earth thought to be driven by mantle flow. This level of perturbation to the dynamic ellipticity or flattening over the past 25 Myr strongly implies a sluggish overturn time.

In addition to the results for the model MF, Fig. 5 also shows time-series of $\Delta H/H$ computed using two additional viscosity profiles, which we label as RW and SC (see Fig. 3). The profile RW, taken from Ricard & Wuming (1991), is inferred from a set of surface geophysical observables related to mantle convection, while the model SC (Steinberger & Calderwood 2006) is additionally constrained using results from mineral physics. In contrast to MF, the profiles RW and SC are not directly constrained by GIA data, although model SC satisfies the so-called 'Haskell average' of mantle viscosity derived from the analysis of ice age data (Mitrovica 1996). The mean perturbation in $\langle \Delta H/H \rangle_{25\mathrm{Ma}}$ obtained from the three time-series in Fig. 5 are shown in Fig. 1(B) (red arrows). These results cluster around the observational constraint of Pälike & Shackleton (2000). [We also computed the mean GIA-induced perturbation, $\langle \Delta H/H \rangle_{3\mathrm{Ma}}$, using models RW and SC. The values we obtained, -1.15×10^{-3} and -1.36×10^{-3}, respectively, are consistent with the prediction based on MF shown in Fig. 1(A).]

The two frames of Fig. 1 define the enigma introduced earlier. No value of ν_{lm} within the family of two-layer viscosity profiles we have adopted can simultaneously reconcile the ice age and mantle convection predictions of changes in the dynamic ellipticity with the bounds estimated by Lourens *et al.* (2001) and Pälike & Shackleton (2000). The ice age predictions (Fig. 1A, blue line) require a relatively weak lower-mantle viscosity to satisfy the bound on $\Delta H/H$ for the past 3.0 Myr, but this class of viscosity models will produce a gross misfit between mantle convection predictions over the past 25 Myr and the associated bound on dynamic ellipticity (Pälike & Shackleton 2000). As an example, while an ice age prediction based on model VM2 falls moderately above the lower bound on $\langle \Delta H/H \rangle_{3\mathrm{Ma}}$ derived by Lourens *et al.* (2001), a convection simulation based on the same viscosity model yields a perturbation to $\langle \Delta H/H \rangle_{25\mathrm{Ma}}$ that is three times higher than the bound on this quantity derived by Pälike & Shackleton (2000). Similarly, the high values of ν_{lm} necessary to reconcile the constraint on the mean value of $\Delta H/H$ over the last 25 Myr derived by Pälike &

Shackleton (2000) (Fig. 1B) will predict an ice age perturbation that is many times higher than the bound inferred by Lourens *et al.* (2001). This is demonstrated by the results based on models MF, RW and SC: While these models yield a convection-induced $\langle \Delta H/H \rangle_{25\mathrm{Ma}}$ that cluster around the observed bound on this quantity, these models predict a GIA-induced mean perturbation $\langle \Delta H/H \rangle_{3\mathrm{Ma}}$ that significantly exceeds the bound provided by Lourens *et al.* (2001).

Not all models considered in Fig. 1 fit the broad suite of GIA and mantle convection data sets that have been used to infer mantle viscosity (Nakada & Lambeck 1989; Lambeck *et al.* 1998; Mitrovica & Forte 2004; Peltier 2004). As an example, while the viscosity models VM2 and MF have been independently inferred by groups analysing GIA data, the two-layer model with $\nu_{\mathrm{lm}} = 10^{23}$ Pa s would grossly misfit most GIA data sets. In regard to Fig. 1(B), model MF provides an excellent fit to data sets connected to mantle convection, for example, long-wavelength geoid harmonics, divergence of horizontal plate motions, dynamic topography and the excess ellipticity of the core–mantle boundary. As a specific example, MF provides an 86 per cent variance reduction of geoid harmonics up to degree and order 32. In contrast, the three lowest viscosity models sampled by the red line in Fig. 1(B) ($\nu_{\mathrm{lm}} = 10^{21}, 3 \times 10^{21}, 10^{22}$ Pa s) increase the variance by 226 per cent, 140 per cent and 33 per cent, respectively, while the two higher viscosity models (3×10^{22} and 10^{23} Pa s) decrease the variance by only 51 per cent and 18 per cent, respectively. That is, models with a constant lower-mantle viscosity of 10^{22} Pa s or less (including VM2) provide a very poor fit to surface observables related to mantle convection.

3 DISCUSSION: RESOLVING THE ENIGMA?

There are at least four possible routes to resolving the enigma described earlier.

First, the results in Fig. 1 may indicate that the viscosity of the mantle is transient; that is, the viscous response to an applied stress is a function of the timescale of the forcing. A flurry of ice age-related papers in the early 1980s considered this possibility (e.g. Sabadini *et al.* 1985), but interest in the topic diminished when no unambiguous evidence of such behaviour emerged in the analysis of GIA data sets and when viscosity profiles were found that could simultaneously reconcile observational constraints associated with GIA and mantle convection (Nakada & Lambeck 1989; Lambeck *et al.* 1998; Mitrovica & Forte 2004).

Second, bounds on $\Delta H/H$ derived from deep-sea sedimentary core records may not be robust. For example, Lourens *et al.* (2004) have highlighted an inaccuracy in the age model adopted by Pälike & Shackleton (2000). Moreover, estimating the stability of Milankovitch frequencies using a time-series that has been pre-tuned to an orbital solution raises the possibility of circular reasoning. This concern was explicitly noted by Pälike & Shackleton (2000) and Lourens *et al.* (2001), though both studies argued that their analysis procedure minimized or avoided the circularity.

Third, tidal dissipation (which also impacts dynamic ellipticity) varies with time (e.g. Hansen 1982; Egbert *et al.* 2004). It is possible that tidal dissipation varied over the last 3 Myr and 25 Myr in the manner necessary to reconcile the enigma (i.e. that changes in the tidal dissipation compensated the geodynamic perturbations to H). [We note that the impact of so-called climate friction on the geological record is thought to be negligible and its contribution can be added as a small perturbation to tidal dissipation parameters (Laskar *et al.* 2004)].

Fourth, it may be possible that earth models exist which yield GIA and convection predictions of $\langle \Delta H/H \rangle$ that are of opposite sign and approximately equal amplitude. The fact that viscosity profiles with significant similarities (MF, RW and SC in Fig. 3) yield a wide range of predictions of $\langle \Delta H/H \rangle_{25\mathrm{Ma}}$ suggests that a search for such models may be warranted.

Insight into these issues may be deepened by taking the calculations described earlier one step further. In particular, to this point we have considered the perturbations in the dynamic ellipticity due to GIA and mantle convection in isolation. However, it is possible that convection may produce an important perturbation to $\Delta H/H$ over the last 3 Myr and that GIA may do the same over the last 25 Myr. We considered the impact of convection on $\langle \Delta H/H \rangle_{3\mathrm{Ma}}$, by taking the average, over only the last 3 Myr, of the 25 Myr model results. For each model, the 3 Myr average was less than 0.08×10^{-3}, and we conclude that the GIA signal dominates $\langle \Delta H/H \rangle_{3\mathrm{Ma}}$.

In Fig. 1(B) we show predictions of the combined GIA and mantle convection signal on the mean perturbation $\langle \Delta H/H \rangle_{25\mathrm{Ma}}$. The GIA signal in this case is first computed by constructing an ice sheet model over the last 25 Myr using the time-series of eustatic sea level variations derived by De Boer *et al.* (2010) (Fig. 4A). Fig. 4(B) shows, in analogy with Figs 2(B) and (C), a prediction of $\Delta H/H$ over the last 25 Myr predicted using viscosity model MF. (The main difference between these calculations and the earlier GIA predictions for the last 3 Myr, is that over the longer time interval we assume that the ocean load variation is geographically uniform. This assumption introduces an error of less than ∼5 per cent in predictions of the mean perturbation to the dynamic ellipticity.) Repeating this GIA calculation for two-layer viscosity profiles and a suite of ν_{lm} values, computing the mean perturbation over the last 25 Myr, and adding the result to the convection-only calculation based on the same viscosity model (red line, Fig. 1B) yields the total (GIA plus convection) predicted perturbation (green line, Fig. 1B). In this case, the magnitude of the GIA contribution is greater than the magnitude of the convection signal for earth models with a lower-mantle viscosity higher than 10^{22} Pa s. This is as one would expect from earlier results; the higher the viscosity, the less complete the isostatic compensation of the ice age surface mass load and the more sluggish the convective flow. We note that while the convection only signal (red line) nearly fits the constraint on $\langle \Delta H/H \rangle_{25\mathrm{Ma}}$ derived by Pälike & Shackleton (2000) for models with $\nu_{\mathrm{lm}} > 3 \times 10^{22}$ Pa s, the combined signal from GIA plus convection only fits this constraint for a band of ν_{lm} values near 10^{22} Pa s.

The results in Fig. 1 do not rule out transient rheology as a mechanism for reconciling the enigmatic observations of the mean perturbation $\langle \Delta H/H \rangle$ over the last 3 Myr and 25 Myr, since distinct viscosity models can be found that fit each data set. However, neither do these results preclude an underestimate of the uncertainty or the presence a bias in the observational constraints based on astronomical tuning. As an example, a factor of two increase in the uncertainty of Fig. 1(A) would allow a model with ν_{lm} values near 10^{22} Pa s to fit both $\langle \Delta H/H \rangle_{3\mathrm{Ma}}$ and $\langle \Delta H/H \rangle_{25\mathrm{Ma}}$; although, as discussed earlier, there is no guarantee that such a model would simultaneously fit independent convection and GIA data sets. Similarly, if an earth model could be found that yielded a cancellation of the ice age and convection perturbations to H, then such a model would also need to simultaneously fit the large database of GIA and convection observables that have been used in past inferences of viscosity.

In any case, the results summarized in Fig. 1 define a rather fundamental enigma in estimates of the Earth's dynamic ellipticity that warrants further attention. A stratigraphic record extending to at

least 30 Ma, characterized by significant Milankovitch periodicities and accurate age constraints, would be key to resolving this enigma. Such a record could be compared with geophysical models to decouple the effects of tidal dissipation, which may vary significantly with time (Hüsing *et al.* 2007), from perturbations in dynamic ellipticity due to GIA and mantle convection. The ultimate resolution of the enigma may lead to a reappraisal of mantle viscosity, a key parameter governing the long-term evolution of the Earth system, or of astronomical calibration or tuning, a methodology that has been used to establish timescales extending through the Cenozoic and into the Mesozoic.

ACKNOWLEDGMENTS

We thank Lucas Lourens and two anonymous reviewers for their constructive reviews of this manuscript.

REFERENCES

Chambat, F., Ricard, Y. & Valette, B., 2010. Flattening of the Earth: further from hydrostaticity than previously estimated, *Geophys. J. Int.*, **183**, 727–732.

De Boer, B., Van de Wal, R.S.W., Bintanja, R., Lourens, L.J. & Tuenter, E., 2010. Cenozoic global ice-volume and temperature simulations with 1-D ice-sheet models forced by benthic δ^{18}O records, *Ann. Glaciol.*, **51**(55), 23–33.

Dziewonski, A.M. & Anderson, D.L., 1981. Preliminary reference Earth model (PREM), *Phys. Earth planet. Inter.*, **25**, 297–356.

Egbert, G., Ray, R. & Bills, B., 2004. Numerical modeling of the global semidiurnal tide in the present day and in the last glacial maximum, *J. geophys. Res.*, **109**, C03003, doi:10.1029/2003JC001973.

Forte, A.M., 2007. Constraints on seismic models from other disciplines: implications for mantle dynamics and composition, in *Treatise of Geophysics*, Vol. 1, pp. 805–854, eds Romanowicz, B. & Dziewonski, A.M., Elsevier, Amsterdam.

Forte, A.M. & Mitrovica, J.X., 1997. A resonance in the Earth's obliquity and precession over the past 20 Myr driven by mantle convection, *Nature*, **390**, 676–680.

Forte, A.M., Quéré, S., Moucha, R., Simmons, N.A., Grand, S.P., Mitrovica, J.X. & Rowley, D.B., 2010. Joint seismic-geodynamic-mineral physical modelling of African geodynamics: a reconciliation of deep-mantle convection with surface geophysical constraints, *Earth planet. Sci. Lett.*, **295**, 329–341.

Hansen, K., 1982. Secular effects of oceanic tidal dissipation on the Moon's orbit and the Earth's rotation, *Rev. Geophys.*, **20**, 457–480.

Hilgen, F.J., Krijgsman, W., Langereis, C.G., Lourens, L.J., Santarelli, A. & Zachariasse, W.J., 1995. Extending the astronomical (polarity) time scale into the Miocene, *Earth planet. Sci. Lett.*, **136**, 495–510.

Hüsing, S.K., Hilgen, F.J., Abdul Aziz, H. & Krijgsman, W., 2007. Completing the Neogene geological time scale between 8.5 and 12.5 Ma, *Earth planet. Sci. Lett.*, **253**, 340–358, doi:10.1016/j.epsl.2006.10.036.

Jiang, X.H. & Peltier, W.R., 1996. Ten million year histories of obliquity and precession: the influence of the ice-age, *Earth planet. Sci. Lett.*, **139**, 17–32.

Kendall, R.A., Mitrovica, J. X. & Milne, G. A., 2005. On post-glacial sea level—II. Numerical formulation and comparative results on spherically symmetric models, *Geophys. J. Int.*, **161**, 679–706.

Lambeck, K., Smither, K. & Johnston, P., 1998. Sea-level change, glacial rebound and mantle viscosity for northern Europe, *Geophys. J. Int.*, **134**, 102–144.

Laskar, J., Joutel, F. & Boudin, F., 1993. Orbital, precessional, and insolation quantities for the Earth from −20 Myr to +10 Myr, *Astron. Astrophys.*, **270**, 522–533.

Laskar, J., Robutel, P., Joutel, F., Gastineau, M., Correia, A.C.M. & Levrard, B., 2004. A long-term numerical solution for the insolation quantities of the Earth, *Astron. Astrophys.*, **428**, 261–285, doi:10.1051/0004-6361:20041335.

Lisiecki, L.E. & Raymo, M.E., 2005. A Pliocene-Pleistocene stack of 57 globally distributed benthic δ^{18}O records. *Paleoceanography*, **20**, PA1003, doi:10.1029/2004PA001071.

Lithgow-Bertelloni, C. & Silver, P.G., 1998. Dynamic topography, plate driving forces and the African superswell, *Nature*, **395**, 269–272.

Lourens, L.J., Wehausen, R. & Brumsack, H.J., 2001. Geological constraints on tidal dissipation and dynamical ellipticity of the Earth over the past three million years, *Nature*, **409**, 1029–1033.

Lourens, L.J., Hilgen, F., Shackleton, N.J., Laskar, J. & Wilson, D., 2004. The Neogene Period, in *A Geologic Time Scale 2004*, pp. 409–440, eds Gradstein, F.M., Ogg, J.G. & Smith, A.G., Cambridge University Press, Cambridge.

Mitrovica, J.X., 1996. Haskell [1935] revisited, *J. geophys. Res.*, **101**(B1), 555–569.

Mitrovica, J.X. & Forte, A.M., 1995. Pleistocene glaciation and the Earth's precession constant, *Geophys. J. Int.*, **121**, 21–32.

Mitrovica, J.X. & Forte, A.M., 2004. A new inference of mantle viscosity based upon a joint inversion of convection and glacial isostatic adjustment data, *Earth planet. Sci. Lett.*, **225**, 177–189.

Mitrovica, J.X., Pan, R. & Forte, A.M., 1994. Late Pleistocene and Holocene ice mass fluctuations and the Earth's precession constant, *Earth planet. Sci. Lett.*, **128**, 489–500.

Mitrovica, J.X., Forte, A.M. & Pan, R., 1997. Glaciation-induced variations in the Earth's precession frequency, obliquity and insolation over the last 2.6 Ma, *Geophys. J. Int.*, **128**, 270–284.

Nakada, M. & Lambeck, K., 1989. Late Pleistocene and Holocene sea-level change in the Australian region and mantle rheology, *Geophys. J. Int.*, **96**, 497–517.

Pälike, H. & Shackleton, N.J., 2000, Constraints on astronomical parameters from the geological record for the last 25 Myr, *Earth planet. Sci. Lett.*, **182**, 1–14.

Peltier, W.R., 2004. Global glacial isostasy and the surface of the ice-age Earth: the ICE-5G (VM2) model and GRACE, *Annu. Rev. Earth planet. Sci.*, **32**, 111–149.

Ricard, Y. & Wuming, B., 1991. Inferring the viscosity and the 3-D density structure of the mantle from geoid, topography and plate velocities, *Geophys. J. Int.*, **105**, 561–571.

Sabadini, R., Yuen, D.A. & Gasperini, P., 1985. The effects of transient rheology on the interpretation of lower mantle viscosity, *Geophys. Res. Lett.*, **12**, 361–364.

Shackleton, N.J., Berger, A. & Peltier, W.R., 1990. An alternative astronomical calibration of the lower Pleistocene time-scale based on ODP Site 677, *Trans. R. Soc. Edinb. Earth Sci.*, **81**, 251–261.

Shackleton, N.J., Crowhurst, S.J., Weedon, G.P. & Laskar, J., 1999. Astronomical calibration of Oligocene-Miocene time, *Phil. Trans. R. Soc. Lond. Ser. A Math. Phys. Eng. Sci.*, **357**, 1907–1929.

Simmons, N.A., Forte, A.M. & Grand, S.P., 2009. Joint seismic, geodynamic and mineral physical constraints on three-dimensional mantle heterogeneity: implications for the relative importance of thermal versus compositional heterogeneity, *Geophys. J. Int.*, **177**, 1284–1304.

Steinberger, B. & Calderwood, A.R., 2006. Models of large-scale viscous flow in the Earth's mantle with constraints from mineral physics and surface observations, *Geophys. J. Int.*, **167**, 1461–1481.